Colloids and Surfaces A: Physicochemical and Engineering Aspects 673 (2023) 131807

Contents lists available at ScienceDirect

Colloids and Surfaces A: Physicochemical and Engineering Aspects

journal homepage: www.elsevier.com/locate/colsurfa

Dopamine-functionalized pectin-based Pickering emulsion as an oral drug delivery system

Jia-qi Zhang [a], Hai-chao Li [b], Jie Wang [c], Sha-sha Liu [a], Jun Li [a], De-qiang Li [a,*]

[a] Xinjiang Key Laboratory of Agricultural Chemistry and Biomaterials, College of Chemistry and Chemical Engineering, Xinjiang Agricultural University, Urumchi 830052, Xinjiang, PR China
[b] Beijing Key Laboratory of Lignocellulosic Chemistry, Beijing Forestry University, Beijing 100083, PR China
[c] CAS Key Laboratory of Colloid, Interface and Chemical Thermodynamics, Beijing National Laboratory for Molecular Sciences (BNLMS), CAS Research/Education Center for Excellence in Molecular Sciences, Institute of Chemistry, Chinese Academy of Sciences, Beijing 100190, PR China

GRAPHICAL ABSTRACT

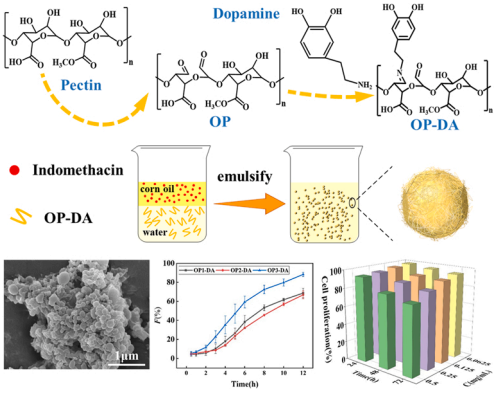

ARTICLE INFO

Keywords:
Pectin
Dopamine
Pickering emulsion
Drug delivery system
Indomethacin

ABSTRACT

Pickering emulsions can be utilized to improve the usage efficiency of water-insoluble drugs as oral drug delivery systems. The present study showed a series of dopamine-functionalized pectin-based Pickering emulsions for anti-inflammatory medication. The dopamine functionalization induced significant differences in wettability, zeta potential, particle size, and PDI value compared with the oxidized pectin. The resultant Pickering emulsions consequently had excellent stability and could be stored for 30 days. Moreover, the morphology of the dried Pickering emulsions was all nano-scale spherical particles. Indomethacin (IND) was used as a water-insoluble drug model. The resultant Pickering emulsion-based drug delivery system showed persistent release of IND for more than 12 h, high pH-responsiveness, and biocompatibility. All the results manifested the excellent potential of dopamine-functionalized pectin-based Pickering emulsions in drug delivery applications. The present work also provided a new approach to preparing Pickering emulsions from modified anionic polysaccharides for delivering the water-insoluble drugs.

* Corresponding author.
E-mail addresses: lsx20131120a@163.com, ldq@xjau.edu.cn (D.-q. Li).

https://doi.org/10.1016/j.colsurfa.2023.131807
Received 10 February 2023; Received in revised form 29 May 2023; Accepted 2 June 2023
Available online 3 June 2023

1. Introduction

Drug delivery system (DDS) is a combination of drugs with carriers via physical or chemical approaches and can implement sustained and controlled drug release in vivo based on the various interactions between drugs and carriers. They can significantly improve the efficacy and safety of drugs by decreasing the drug release rate and expanding the duration [1]. Drug-loaded microcapsules are excellent representatives that can release drugs under specific conditions and protect the drugs from external damage [2]. The emulsion template method [3], microfluidic method [4], precipitation polymerization [5], and interfacial polymerization [6] are commonly used.

Pickering emulsion templates have been developing rapidly due to their advantages in operation, safety, and sustainability [7]. Single or multilayer interfacial film-stabilized emulsions are formed through the absorption of micro- and nano-solid particles on the oil-water interface. In addition, the adsorption of particulate emulsifiers tends to be slow and irreversible [8]. The particulate emulsifier forms a dense protective layer on the surface of the water-oil interface without causing a significant reduction in the interfacial tension [9]. Hence Pickering emulsion templates have the advantages of an irreversible adsorption interface, high coalescence stability, and stable droplet size compared to conventional emulsions [10,11]. Moreover, the irreversible physical adsorption without adding other crosslinkers determined the superiority in operation and safety [12]. Therefore, oil-in-water Pickering emulsions can potentially encapsulate the water-insoluble drugs in the oral drug delivery system.

Water-insoluble drugs have excellent biological activities but are limited by their poor water solubility, chemical stability, and bioavailability [8]. To this end, oil-in-water Pickering emulsions have been employed as carriers for delivering water-insoluble drugs [13]. Natural polymers, including pectin, alginate, chitosan, cellulose, and starch [8,14], have received significant attention as Pickering stabilizers and emerged with enormous potential. Unlike other polysaccharides, pectin possesses specific biological activities such as probiotics, hypocholesterolemia, hypoglycemic, and anticancer effects [15]. Thus, pectin may be one of the ideal candidates for the preparation of drug delivery systems if it can be used as a solid particle for Pickering emulsions.

In recent years, pectin-protein complex has been used as a particulate emulsifier for Pickering emulsions [16]. The resultant emulsions were typically stabilized by reducing the interfacial tension between water and oil phases and forming an interface layer that prevents the electrostatic interaction between oil droplets [8]. Generally, the interfacial adsorption was considered sluggish and irreversible for particles with near-neutral wettability (i.e., $\theta_{o/w}$ =90°) [17]. However, the electron-rich functional groups (e.g., hydroxyl and carboxyl groups) result in pectin being highly hydrophilic and exhibiting poor stabilizing properties for Pickering emulsions. Nitrogen-containing macromolecules can significantly regulate the wettability of pectin molecules via electrostatic interaction and hydrogen bonding, such as gliadin [18], plant protein [19,20], casein [21], lipoprotein [22], whey protein [23]. In this process, the negatively charged carboxyl functional groups were coupled with the amino, imino, and acylamino groups [24,25]. Moreover, hydrogen bonding caused the coupling of the hydroxyl and nitrogen-containing groups [26]. The hydrophilia of pectin consequently decreased, and the resultant composites could be used as stabilizers to form stable Pickering emulsions. However, the non-covalent interactions between the electron-rich functional groups and nitrogen-containing functional groups can be facilely broken, resulting in the disintegration of composites [26]. Thus, the fabrication of pectin derivatives that have nitrogen-containing groups via chemical routes may not only decrease the hydrophilia but also possess stability. These pectin derivatives may be consequently favored to form stabilized Pickering emulsions.

The hydroxyl and carboxyl functional groups in the pectin molecules are deservedly the reaction sites for chemical modification such as esterification, amidation, etherification, acetylation, oxidation, etc. [15]. Most of the reactions occurred in the presence of toxic catalysts such as Dicyclohexylcarbodiimide/N-hydroxysuccinimide (DCC/NHS) and N-(3-Dimethylaminopropyl)-N′-Ethylcarbodiimide Hydrochloride/N-hydroxysuccinimide (EDC/NHS), from which the added catalysts need to be removed via the fussy routes; otherwise, the residual catalysts may appear their toxic side effects on subsequent biomedical applications. Periodate has been widely used to oxidate vicinal diols of the polysaccharides to dialdehyde groups that are the reaction sites for Schiff's base reaction [27]. Dopamine (DA), an important neurotransmitter, can bind extrasynaptic receptors via volume transmission to achieve the role of the extrasynaptic messenger molecule. It is a contraction of 3, 4-dihydroxyphenethylamine that can spontaneously oxidate to dopamine quinone and further convert to polydopamine (PDA) [28]. PDA functionalization has been considered a material surface chemistry-independent route, which has been consequently used to regulate the surface chemistry of materials for drug delivery applications [29]. For periodate-oxidized pectin, the DA can not only couple with the negatively charged carboxyl functional groups but also react with aldehyde groups via Schiff's base reaction. Moreover, the formed imine linkages can also couple with carboxyl functional groups due to the electron-rich nature of nitrogen [30].

The present study developed a series of Pickering emulsions stabilized by dopamine-functionalized pectin, which were further used as drug delivery systems. The effect of dopamine functionalization on the chemical structure, wettability, zeta potential, and particle size was studied. Moreover, the stability and creaming index of Pickering emulsions were determined. Indomethacin was selected as the water-insoluble drug model to calculate the release performance of emulsion-based drug delivery systems. The biocompatibility of the obtained emulsions was also determined.

2. Materials and methods

2.1. Materials

Pectin and dopamine hydrochloride were provided by Shanghai Macklin Biochemical Co., Ltd. (Shanghai, China). The degree of esterification of pectin is 27.3%, and its average molar weight is 37.2 kDa. The sodium periodate ($NaIO_4$), absolute ethanol, and ethanediol were purchased from Tianjin Yongsheng Fine Chemicals Co., Ltd. (Tianjin, China). The HCl (aq), NaOH, NaH_2PO_4, and Na_2HPO_4 were purchased from Sinopharm Chemical Co., Ltd. (Shanghai, China). Corn oil was produced by Cofco Fulinmen Food Co. Ltd. (Tianjin, China). All chemicals were directly used without pretreatment.

2.2. Preparation of oxidized pectin (OP)

The oxidized pectin was produced according to our published data [31]. In detail, pectin (10 g) was added to 75 mL of ethanol with slow stirring, followed by adding 300 mL of distilled water and stirring until the pectin was fully dissolved. Sodium periodate (3 g) was dissolved in 50 mL of distilled water, which was added to the pectin solution at room temperature under dark conditions with stirring for 2 h. Then, excess ethanediol (2 mL) was added to terminate the oxidation reaction. The resultant solution was centrifuged at 10,000 rpm, dialyzed, and freeze-dried to obtain the final OP. The obtained OP had an oxidation degree of 38.43%, which was determined according to the published method [32].

2.3. Preparation of Pickering emulsions stabilized by dopamine-functionalized OP (OP-DA)

Three groups of 4 wt% OP solutions were obtained, and their pH were adjusted to 1, 2, and 3 by adding HCl solution (0.1 mol/L). The surface negative charge of OP contributed to high surface energy that

was not conducive to the stability of Pickering emulsions. Thus, we prepared OP-DA composite solutions by adding DA into the OP solutions according to the 1:1 molar ratio of the aldehyde group to the amino group. The obtained particles were noted as OP1-DA, OP2-DA, and OP3-DA, viz., the numbers 1, 2, and 3 represented the pH of the preparation conditions. This process was performed under dark conditions to delay the oxidative auto-polymerization of DA.

The OP-DA composites-stabilized Pickering emulsions were obtained at different water/oil ratios (3:7, 4:6, 5:5, 6:4, 7:3, v/v), and the total volume of emulsions was 10 mL. Briefly, corn oil and OP-DA suspension were mixed in a glass bottle (20 mL) with preset water-oil ratios and severely sheared by a FSH-2A high-speed homogenizer at 10,000 rpm for 5 min. The obtained Pickering emulsions were sealed and kept quiescently at room temperature. A small dosage of emulsions was added to the corn oil or distilled water to judge the type of emulsions. Results showed good dispersion in distilled water and agglomeration in oil, indicating the oil-in-water Pickering emulsion. The obtained emulsions from the OP-DA under different pH conditions were noted as OP1-DAPE, OP2-DAPE, and OP3-DAPE (Fig. 1).

2.4. Preparation of the emulsion-based DDS

The indomethacin-loaded DDS were further prepared according to the preparation process of Pickering emulsions. Indomethacin powder (IND) was added to corn oil by magnetic stirring to dissolve it, resulting in an oil phase with a concentration of 3 mg/mL. The other operations were performed as same as the preparation of Pickering emulsions. The obtained IND-loaded Pickering emulsions were noted as OP1-DA/IND, OP2-DA/IND, and OP3-DA/IND.

2.5. Characterization

2.5.1. FT-IR and ^{1}H NMR analysis

FT-IR technology was used to characterize pectin, dopamine, OP, and OP-DA. Generally, the samples were mixed with KBr and pressed into a flake. The resultant slices were scanned by an FT-IR spectrometer (IRAffinity-1, Shimadzu, Japan) in the 4000–500 cm^{-1} wavenumber range with 32 scans and a resolution of 4 cm^{-1}. ^{1}H NMR spectra was used to characterize the DA functionalization of OP on Bruke AVANCE NEO 500 nuclear magnetic resonance spectrometer at 25 °C, using deuteroxide (D_2O) as solvents, and maleic acid (MA) was used as the internal standard. In this process, 6 mg of maleic acid and 12 mg of OP-DA were used. The grafting efficiency (GE) was calculated by the following equations.

$$\mathrm{GE}\ (\%) = \frac{m_{DA}}{m_{OP-DA}} = \frac{m_{MA} \times 4 \times I_{PhH} \times 189.64}{m_{OP-DA} \times 3 \times I_{MAH} \times 116.07} \times 100 \quad (1)$$

where 189.64 and 116.07 were the molecular weight of DA and MA, respectively. I_{PhH} and I_{MAH} stand for the integral areas of the aromatic proton of DA and alkene proton of MA, and the proton number of aromatic and alkene protons were 4 and 3. The m_{MA} and $m_{OP\text{-}DA}$ were respective to the dosage used in the quantitative NMR characterization.

2.5.2. Three-phase contact angle

The three-phase contact angle of OP and OP-DA was determined by an optical contact angle & interface tension meter (SL200KB, KINO Industry Co., Ltd., USA) [33]. Briefly, the lyophilized OP and OP-DA powder were pressed into cylindrical tablets with a diameter of 8 mm and thickness of 2 mm at a pressure of 2 MPa. Then, the tablets were placed into a glass beaker containing an oil phase. Later, 2.5 μL of

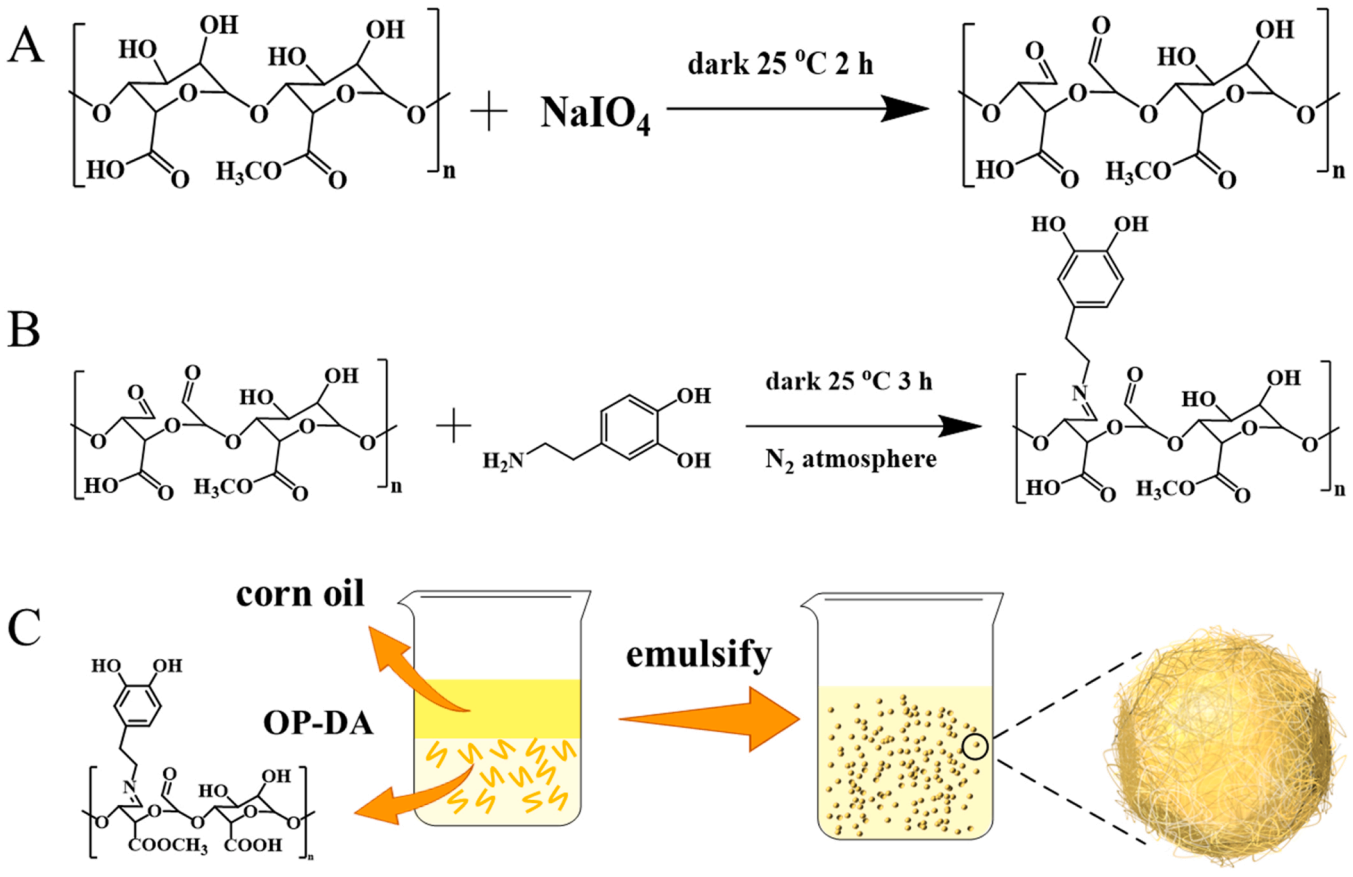

Fig. 1. Schematic illustration of the preparation process. (A) The oxidation of pectin by sodium periodate; (B) Schiff's base reaction between OP and DA; (C) Preparation of Pickering emulsion stabilized by OP-DA.

distilled water was dropped on the surface of the slice by a microsyringe. The process of dripping was shot by a video camera. CAST3.0 built-in software was employed to fit the droplet outline to determine the contact angles between water and slices.

2.5.3. Particle size, polydispersity index (PDI), and zeta potential of OP and OP-DA

The particle size, zeta potential, and PDI of OP and OP-DA were determined by Zetasizer Nano (Zetasizer Nano-ZS, Malvern Instruments Ltd., UK) [23]. Each measurement was repeated three times at room temperature, with the averages provided. The dynamic light scattering technique was used for particle size and PDI measurements in a 12 mm cell. For zeta potential, all samples were sonicated for 5 min. Laser Doppler velocimetry was employed to determine the electrophoretic mobility of the pretreated samples, and the zeta potential was fitted by the Smoluchowski equation.

2.5.4. Visual appearance and long-term storage stability of emulsions

The OP-DA stabilized Pickering emulsions were prepared according to Section 2.3. The obtained emulsions were stored in glass bottles at room temperature for 30 days. The visual appearance of the emulsions was recorded on the 1st and 30th days. To calculate the emulsion stability, the creaming index (CI, %) was measured according to Eq. (2).

$$CI(\%) = \frac{H_c}{H_t} \times 100 \tag{2}$$

where H_c (cm) was the height of the cream, and H_t (cm) was the initial height of the emulsion.

2.5.5. Optical microscopy

According to the published data [34,35], polarized optical microscopy (MX-117PS, Shenzhen Obvious Optics Co., Ltd, China) with a Toupcam microscope camera (16 million pixels) was used to characterize the non-polarizing microscope images of the Pickering emulsions in a bright field. Briefly, 1 mL of emulsions was added to a 10 mL sample bottle, followed by adding 9 mL of deionized water, which was dispersed on a vortex mixer. The dilute emulsions were dropped on a micro slide, then covered with a coverslip, and observed. This process was performed at room temperature, and the magnification of the microscope was × 40.

2.5.6. Scanning electron microscopy (SEM)

The OP2-DAPE and OP2-DA/IND were dropwise added on a silicon plate and vacuum dried in an oven at 60 °C. The tailored samples were pasted on the microscope stage with conductive adhesives, which were further sprayed with gold for 5 min. The microtopography of the samples was scanned by a scanning electron microscope (SEM, Hitachi S-4800, Japan) with an acceleration voltage of 1–10 kV and an in-lens detector.

2.6. In vitro drug release testing and kinetics study

NaH_2PO_4-Na_2HPO_4 buffer with different pH were used as the release mediums. The pH of the buffer solutions were adjusted by NaOH and HCl solution (0.1 mol/L) to 1.2, 6.8, and 7.4, which were the simulated gastric fluid (SGF), small intestinal fluid (SSIF), and colon fluid (SCF). The standard curves of IND for different release mediums were tested, with R^2 of 0.9992, 0.9998 and 0.9991 for pH= 1.2, PH= 6.8 and pH= 7.4, respectively (Fig. S1). The effect of release time on the cumulative release ratio was studied in different simulated fluids to obtain the sustained-release performance of IND-contained Pickering emulsions. A specific dose of emulsions was injected into the dialysis bag that was placed in a beaker containing 50 mL simulated mediums (i.e., SGF, SSIF, and SCF). The release experiments were performed at 37 °C. Four milliliters of release medium were sucked out at regular intervals, centrifuged at 8000 rpm, and filtrated by a millipore filter (0.22 μm). Four milliliters of the corresponding buffer solution were immediately added to the release medium when the release medium was sucked out. The concentration of IND in the release medium was determined by a UV-Vis spectrophotometer at 320 nm, and the cumulative release ratios at time t were calculated by the following equation.

$$F(\%) = \frac{C_n \times V_0 + V_i \sum_{i=1}^{n-1} C_i}{m} \times 100 \tag{3}$$

where F (%) and m (mg) represented the cumulative release ratio and the total loading of IND, the C_n (mg/L) and C_i (mg/L) were the concentration of IND in the release medium after the nth and ith samplings, V_i (mL) and V_0 (mL) were the volumes of sampling and release medium.

To better describe the release behavior of IND from the IND-loaded emulsions, kinetic studies were performed to fit the data of release experiments. The first-order model (Eq. (4)), Higuchi model (Eq. (5)), the Ritger-Peppas model (Eq. (6)), and the Bhaskar model (Eq. (7)) were the commonly used kinetic models and have been consequently used in the present study.

$$-\ln(1-F) = k_1 t \tag{4}$$

$$F = k_2 t^{0.5} \tag{5}$$

$$\ln F = n \ln t + \ln k_3 \tag{6}$$

$$-\ln(1-F) = k_4 t^{0.65} \tag{7}$$

where n is the diffusion index that determines the type of diffusion mechanism, and k_i were the kinetic constants of different models.

2.7. Cytotoxicity assay

A professional institution, Shanghai Bingxin Biotechnology Co., LTD (China), was employed to perform the cytotoxicity assay. The influence of OP-DAPE on the L929 fibroblast proliferation was used to calculate the cytotoxicity by a colorimetric assay based on 3-(4, 5-dimethylthiazol-2-yl) 2, 5-diphenyl tetrazolium bromide (MTT). A hundred microliters of L929 fibroblast cells (8×10^4 cells /mL) were inoculated on a 96-well plate and incubated overnight in an incubator at 37 °C under 5% CO_2 atmosphere. The operating fluids with different OP-DA concentrations (1, 0.5, 0.25, 0.125, and 0.0625 mg/mL) were obtained by mixing OP-DA with a complete culture solution containing 90% minimum essential medium (MEM, Hyclone, Thermo Fisher Scientific, USA) and 10% fetal bovine serum (FBS, Gibco, Thermo Fisher Scientific, USA). Then, a hundred microliters of culture solution were accordingly added to each well, and the cells were incubated at 37 °C under 5% CO_2 atmosphere for 24, 48, and 72 h. The absorbance of the cell at different time intervals was determined at 570 nm by a microplate reader (Thermo Scientific, Multiskan Spectrum), and the cell proliferation ratios were calculated as follows.

$$\textit{Cell proliferation ratio}\ (\%) = \frac{\text{The OD value of the sample}}{\text{The OD value of the control group}} \times 100 \tag{8}$$

In addition, the cultured cells were observed by IX71 fluorescence microscopy (Olympus Corporation, Japan) to observe cell proliferation visually. The cell culture process was according to the above operations, and the cell proliferation in the solution containing OP1-DAPE (0.0625 mg/mL) was collected as the representative. One milliliter of the corresponding staining solution was added to each well, and the incubation was continued for 15 min. The live cells (yellow-green fluorescence) and dead cells (red fluorescence) were detected simultaneously using an excitation filter (490 ± 10 nm) on the fluorescence microscope.

3. Results and discussions

3.1. Characterization

3.1.1. Chemical characterization

The periodate oxidation of vicinal diols and Schiff base reactions have presented high popularization and efficiency in the functionalization of pectin [14,15,27,31]. Thus, we just employed the FT-IR to analyze the chemical variation among pectin, OP, DA, and OP1-DA, and the results are shown in Fig. 2A. The stretching vibrations of C═O of carbomethoxy groups, C-O linkage of the secondary alcohol, and C═O of free carboxyl groups in pectin molecules can be found at 1746, 1072, and 1649 cm^{-1} [31]. Compared with the native pectin, the wide vibration peak at 1649 cm^{-1} shifted to 1609 cm^{-1}, which was ascribed to the enol tautomers evaluated from the formyl groups. Moreover, the absorption peak at 1072 cm^{-1} almost disappeared in OP. These changes could prove that the *o*-hydroxyl group of the pectin molecule was oxidized. For FT-IR spectra of DA, the peaks located at 1504 cm^{-1} and 1616 cm^{-1} were the C═C resonance vibrations of the aromatic ring and bending vibration of N-H [36]. Unlike OP and DA, the FT-IR spectra of OP1-DA showed a new shoulder peak on the left of the peak at 1640 cm^{-1}, which was ascribed to the characteristic absorption peak of the imine bond, indicating the successful Schiff's base reaction.

Quantitative ^{1}H NMR was employed to prove Schiff's base reaction between the OP and DA, and the results are shown in Fig. 2B. The sharp singlet at 3.67 ppm was ascribed to the protons in the methoxy groups of the esterified pectin. The little peaks on the yellow background represented the H-1 (5.04 ppm), H-2 (3.94 ppm), H-3 (4.06 ppm), H-4 (4.32 ppm), and H-5 (4.82 ppm) in the D-galacturonic acid unit, respectively [37,38]. Moreover, the peak at 3.51 ppm represented the H-1′ in the oxidized pectin unit due to the presence of electron-absorbing functional groups on both sides. The characteristic peaks of DA residue can be found at 2.72 ppm (H), 3.07 ppm (G), 6.59 ppm (D), 6.68 ppm (C), and 6.74 ppm (E). Moreover, the grafting efficiency was determined as 40.49%.

3.1.2. Three-phase contact angle

Wettability is one of the vital capabilities of particles that can form a Pickering emulsion. Thus, the wettability properties of OP and OP-DA were calculated separately on lyophilized samples, and the three-phase contact angles ($\theta_{o/w}$) of OP and OP-DA are shown in Fig. 3. The $\theta_{o/w}$ values of OP prepared at different pH conditions were in the range of 65.14° to 76.72°, indicating that OP can be employed as a particulate stabilizer for forming Pickering emulsions. However, the $\theta_{o/w}$ values obviously decreased with the increased pH, indicating an increasing surface free energy. This phenomenon was due to the protonation of carboxyl functional groups, viz., the lower proton concentration contributed to the ionization of carboxyl functional groups [39], and the OP consequently showed lower contact angles.

The DA-functionalization induced a slight increase in the wettability of the OP, which ranged from 67.31° to 79.37°. It was due to the non-covalent interactions between carboxyl and imine groups, which were competing with protonation. Moreover, phenolic hydroxyl groups in the DA molecules dissociated in alkaline and near-neutral mediums but remained under acidic conditions [40]. Thus, the OP-DA showed higher $\theta_{o/w}$ values than the OP prepared at the same pH conditions. Interfacial adsorption was generally considered sluggish and irreversible for particles with near-neutral wettability ($\theta_{o/w}$ =90°) [17]. Thus, the OP-DA contributed to obtaining more stable Pickering emulsions than OP under the same pH condition.

3.1.3. Zeta potential, particle size, and polydispersity index (PDI) of OP and OP-DA

In addition to the wettability, the zeta potential, particle size, and PDI are also essential indices to measure the stabilizing capacity of the particulate stabilizers. Therefore, these indices of the obtained granules were determined, and the results are shown in Table. S1 (Supporting information). The zeta potential of all the OP samples was negative, which was an inherent characteristic of anionic macromolecules. Moreover, the OP-DA showed a positive zeta potential, indicating the electrostatic interactions between the dissociated carboxyl and imine groups. These results manifested that electrostatic attraction exceeded the repulsive force, and the pectin chains tended to condense in the emulsions. For a branched polymeric compound, it favored the chain entanglement and the consequent formation of stable Pickering emulsions. The solid particles need to have a particle size in the range of a few microns to tens of microns, and the gravity effect can be ignored for particles with a 2 μm grain diameter [41]. In the present study, all the samples possessed an average grain diameter below 3.5 μm, indicating the stabilization capability for forming Pickering emulsions. Under different pH conditions, the particle size of OP gradually decreased with the increase in pH. The reason for this may be that the particle tended to be more stable when it was close to pKa, and PDI of the particle also decreased with the increase of pH of the system. The PDI values of all samples ranged from 0.358 to 0.896. Compared with the published data that used pectin/zein as the solid particles [34], the Pickering emulsions that used OP as stabilizers showed a wider diversity of particle size due to the electrostatic interaction [33]. The pKa of the pectin was about 3.5. Therefore, the -COOH existed as $-COOH_2^+$ when the pH of the preparation condition were 1 and 2. The electrostatic attraction caused particle

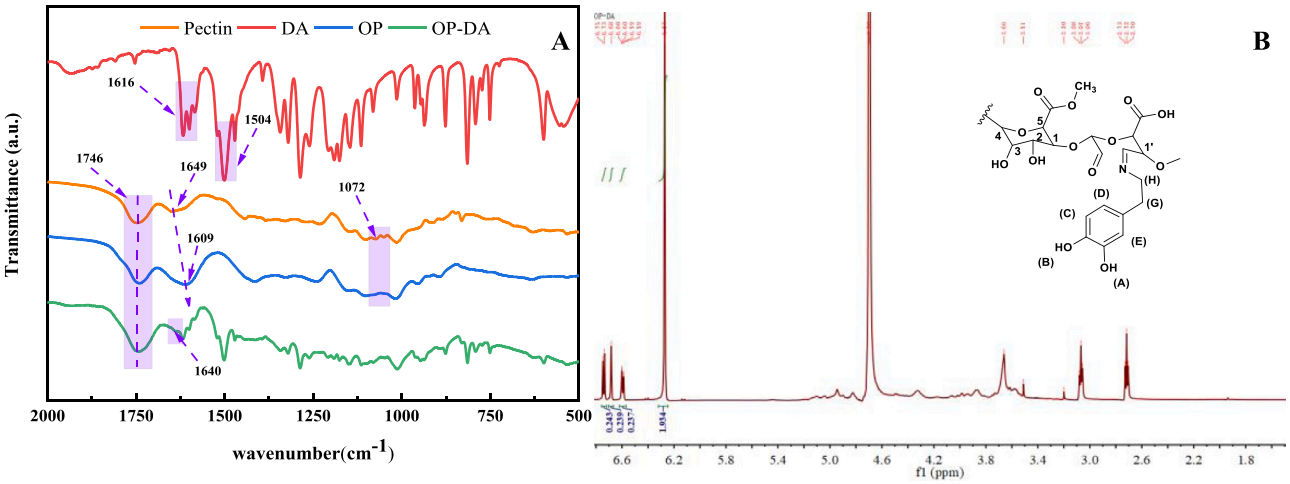

Fig. 2. Chemical characterization. (A) FTIR spectra of the DA, pectin, OP, and OP-DA; (B) quantitative NMR spectra of OP2-DA.

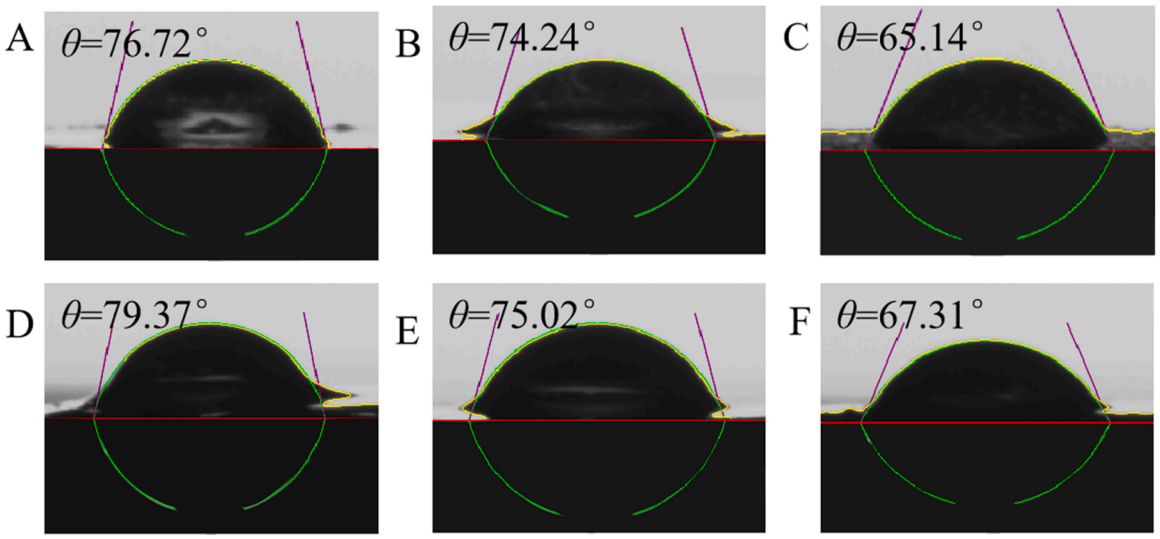

Fig. 3. Oil-in-water three-phase contact angles ($\theta_{o/w}$) of the OP1(A), OP2(B), OP3(C), OP1-DA(D), OP2-DA(E), and OP3-DA(F).

movement, resulting in larger particle size and PDI value [18,42,43]. The pH condition of OP3 was close to the pKa of the pectin, and OP3 consequently presented a smaller particle size and PDI than OP1 and OP2. Moreover, the PDI values of OP1-OP3 were all higher than 0.5, indicating an unstable state of the resultant Pickering emulsion. The PDI values of OP-DA decreased with the increasing pH of the preparation process, which confirmed the importance of charge shielding. The PDI values also illustrated that the surface modification of OP significantly decreased the particle-size diversity. Thus, the sample OP1-DA and OP2-DA presented low PDI values of 0.358 ± 0.032 and 0.416 ± 0.031, indicating excellent stabilization capability. Comparing the PDI values of OP1-OP3, that of OP1-DA, OP2-DA, and OP3-DA significantly decreased to below 0.5, showing the efficacy of DA-functionalization. These results showed that the DA-functionalization significantly regulated the zeta-potential, particle size, and PDI of OP, and the obtained OP-DA accordingly presented better stabilization capability than OP.

3.1.4. *Visual appearance and long-term storage stability*

Fig. 4 shows the visual appearance and storage stability of the Pickering emulsions that were prepared with various oil/water ratios under different pH conditions. The emulsifying volume increased with the increased oil volume fraction ranging from 0.3 to 0.7. This result was consistent with the published data [44]. Moreover, the emulsifying volume ratios were above 90% when the oil phase fraction in OP-DAPE ranged from 0.5 to 0.7. The emulsifying ability of the OP-DA decreased with the increased pH. The OP can react with dopamine via the electrostatic attraction or Schiff's base reaction. In particular, the lower pH condition contributed to the electrostatic attraction and inhibited Schiff's base reaction, which consequently decreased the hydrophilicity of OP-DA [45]. The results can also be proved by the wettability (Fig. 3).

The storage stability of the emulsions was calculated after 30 days of storage. The emulsions were converted into emulsion gels, which improved their long-term stability [34]. Moreover, the emulsifying volume fractions changed slightly compared with the initially prepared

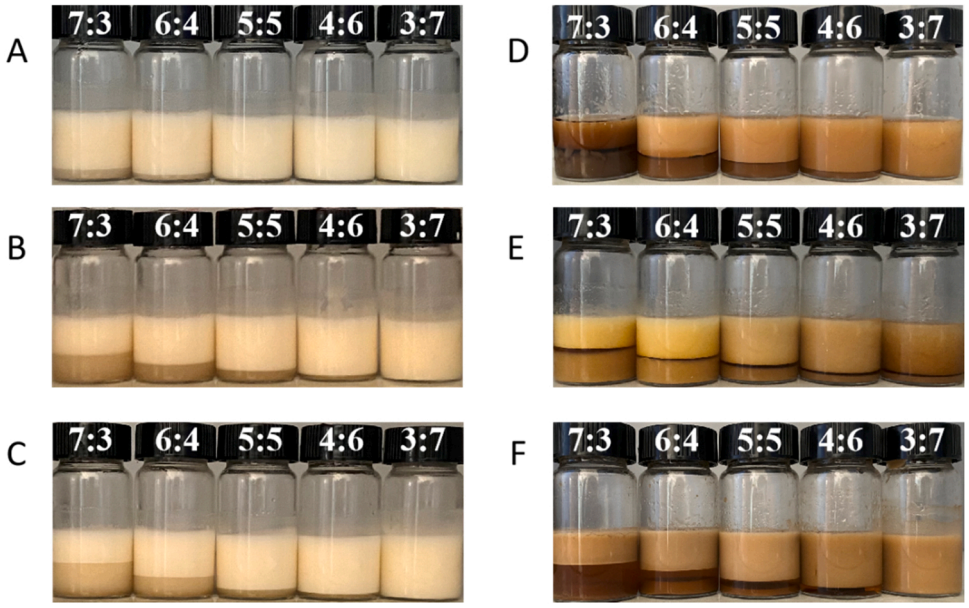

Fig. 4. Visual appearance of Pickering emulsions prepared under different pH conditions with various water/oil ratios. Storage for 1 h (A-C) and 30 days (D-F), where A and D were the emulsions prepared at pH= 1, B and E at pH= 2, and C and F at pH= 3, respectively.

OP-DAPE. CI can be used to calculate storage stability [46]. In the present study, the CI values were approximately 90% when the oil phase fraction was 0.6 or 0.7 (Fig. S2), indicating excellent storage stability. It was also significant that the color of the emulsions changed to brown. This transformation was due to the auto polymerization of dopamine, viz., the polydopamine, a biocompatible material, was obtained during the storge because of UV irradiation [47]. The electrostatic interaction, Schiff's base reaction, and auto polymerization ensured the excellent storage stability of the emulsion systems.

3.1.5. Optical microscopy analysis

Optical microscope can be used to observe the shape and state of the emulsion droplet of the OP-DAPEs. Fig. 5 shows the morphology of OP-DAPEs stored at room temperature for 30 min and 30 days. Overall, the droplet of all the samples showed a regular spherical shape with a micron size. The emulsion droplet size increased as oil phases increased by comparing the influences of different water-oil ratios. This phenomenon is consistent with the findings of Arditty et al. [48]. Limited coalescence may occur during the preparation process, which is determined by the volume fraction of the dispersed phase and the number of particles. When the total interfacial area of the oil phase exceeded the interfacial area covered by the solid particles in the emulsion system, the oil droplets rapidly coalesced into larger droplets, reducing the water-oil interfacial area and increasing the stability of the emulsion. Moreover, the pH did not significantly influence the diameter of emulsion droplets under the same water/oil ratio condition (Fig. 5A-C and D-F). The results differed from the pectin/zein Pickering emulsions fabricated by Zhang et al. [49]. It may be caused by the significant difference in water solubility. They also confirmed that the pectin with a higher methylation degree possessed better adaptability to the pH (i.e., ion strength), viz., free carboxyl groups would induce the change in diameter of emulsions droplets. In the present study, the amino groups in dopamine existed as the $-NH_3^+$ under acidic conditions, which can be attracted by carboxyl groups in the pectin chain. This electrostatic interaction could shield the carboxyl groups in the pectin chain, resulting in an insensitivity to pH. Fig. 5D-F present the shape and state of the emulsion droplet of the OP-DA stored for 30 days, and there was no apparent difference compared with the emulsions stored for 30 min. These results manifested the stabilization capability of OP-DA to form Pickering emulsions.

3.1.6. SEM analysis

The morphology of the OP2-DAPE and drug-loaded OP-DAPE microspheres (i.e., OP2-DA/IND) was obtained by the SEM technique, which is shown in Fig. 6 with a magnification of 10, 000. The OP2-DAPE appeared as nano-scale spherical particles but was inhomogeneous and reunited, as well as the OP2-DA/IND. These results indicated the stability of OP2-DAPE and the slight influence of IND loading. The particle size of OP-DAPE shown in the SEM image was much smaller than that from optical microscopy (Fig. 5). This is because the pectin chain was flexible, which was much different from the rigid particles, such as silica microspheres, cellulose nanocrystals, and polystyrene microspheres. Thus, the resistance of pectin molecular chains to surface forces was much lower than that of rigid nanoparticles during the drying process, and the as-prepared microcapsules collapsed. The morphological analyses indicated that the microspherical materials could be obtained via the Pickering emulsion route.

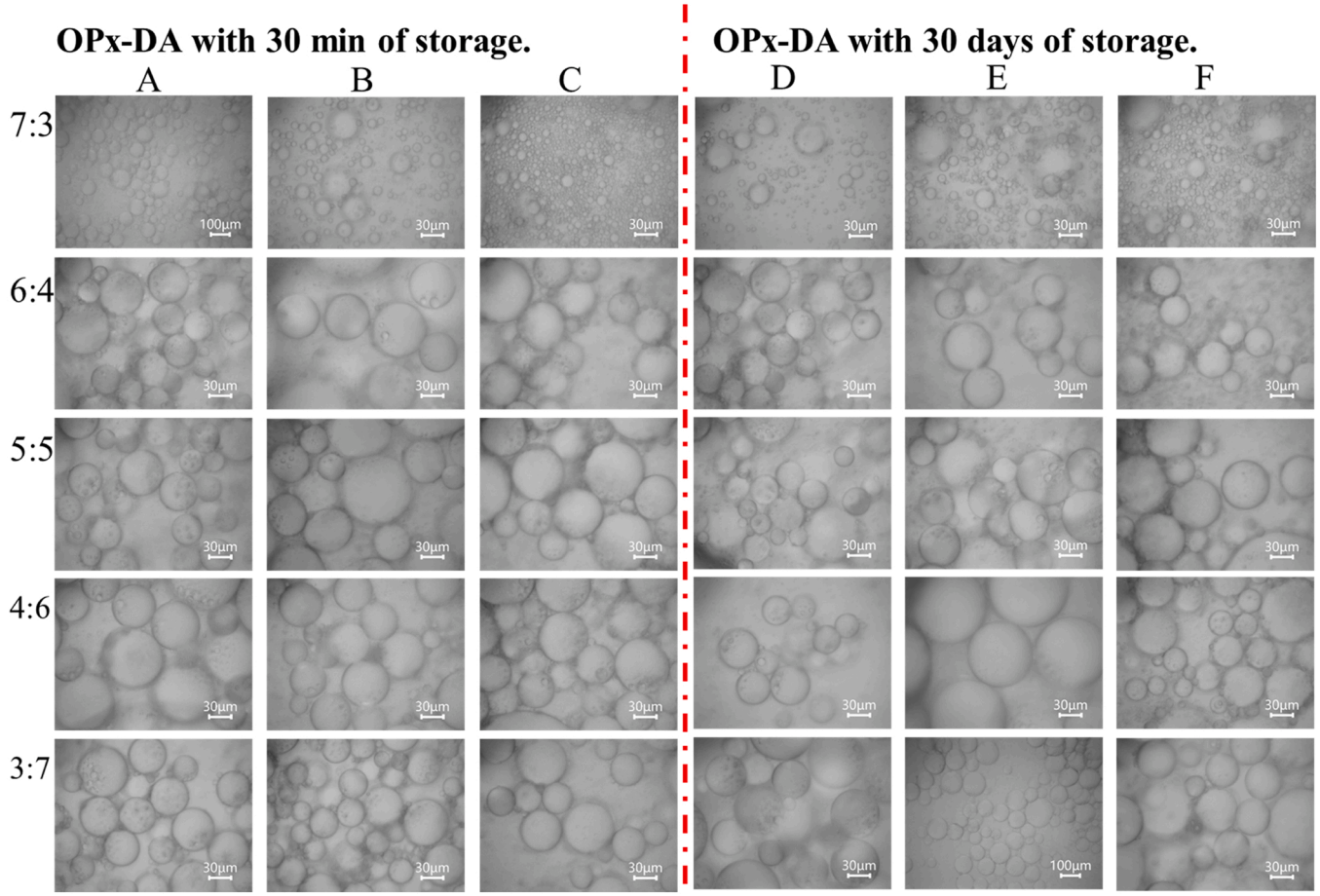

Fig. 5. Optical microscopic images of OPx-DA with different oil/water ratios. (A and D) OP1-DAPE; (B and E) OP2-DAPE; (C and F) OP3-DAPE.

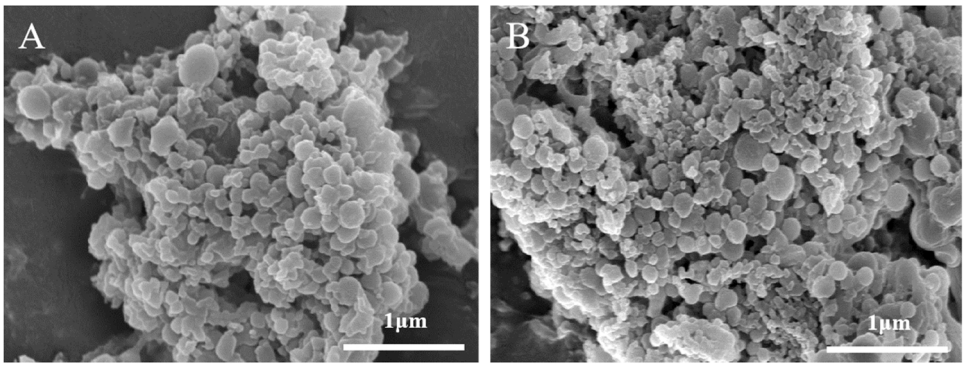

Fig. 6. SEM images of the (A) OP2-DAPE and (B) drug-loaded OP2-DAPE (i.e., OP2-DA/IND).

3.2. *In vitro drug release and kinetics study*

IND is commonly used for rheumatoid arthritis and non-rheumatoid inflammatory diseases but showed low bioavailability [14]. At the same time, it has chemoprotective effects against colon cancer [50]. Many researchers have attempted to encapsulate IND in natural and synthetic polymer systems to preserve the gastrointestinal tract from adverse mucosal injury [51]. The present study prepared oil-in-water emulsions to contain hydrophobic indomethacin, and the sustained release performance of DDS was calculated. The present study employed OP-DAPE to fabricate DDS and calculate its sustained release performance. All the results are shown in Fig. 7. It can be seen that all DDSs sustained IND release for more than 12 h. In contrast to the sustained release of IND power in the release medium in previous studies, the emulsion-based DDSs were able to effectively prolong the release of IND.

All the DDSs showed a low cumulative release ratio of less than 7% in the first 2 h under SGF conditions. These results confirmed that the drug was fractionally released in the acidic medium, which was conducive to the drug reaching the lesion. This phenomenon was according to the stability of the IND itself and the resultant OP-DAPE under acidic conditions. Similar results have also been obtained in the SSIF, and all the DDSs released less than 10% IND in 6 h. The DDSs presented different

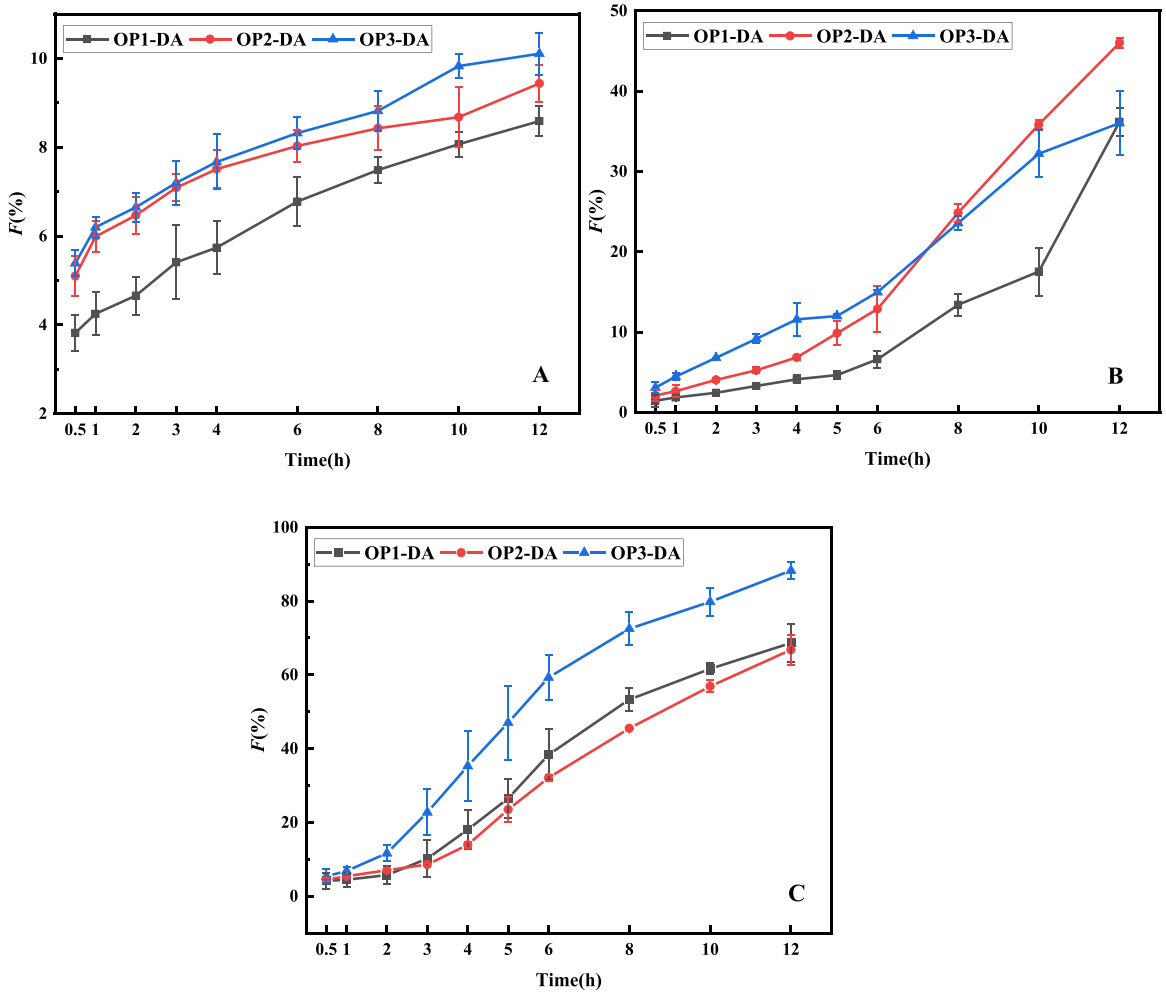

Fig. 7. Cumulative release ratios under different pH conditions, (A) pH= 1.2; (B) pH= 6.8; (C) pH= 7.4.

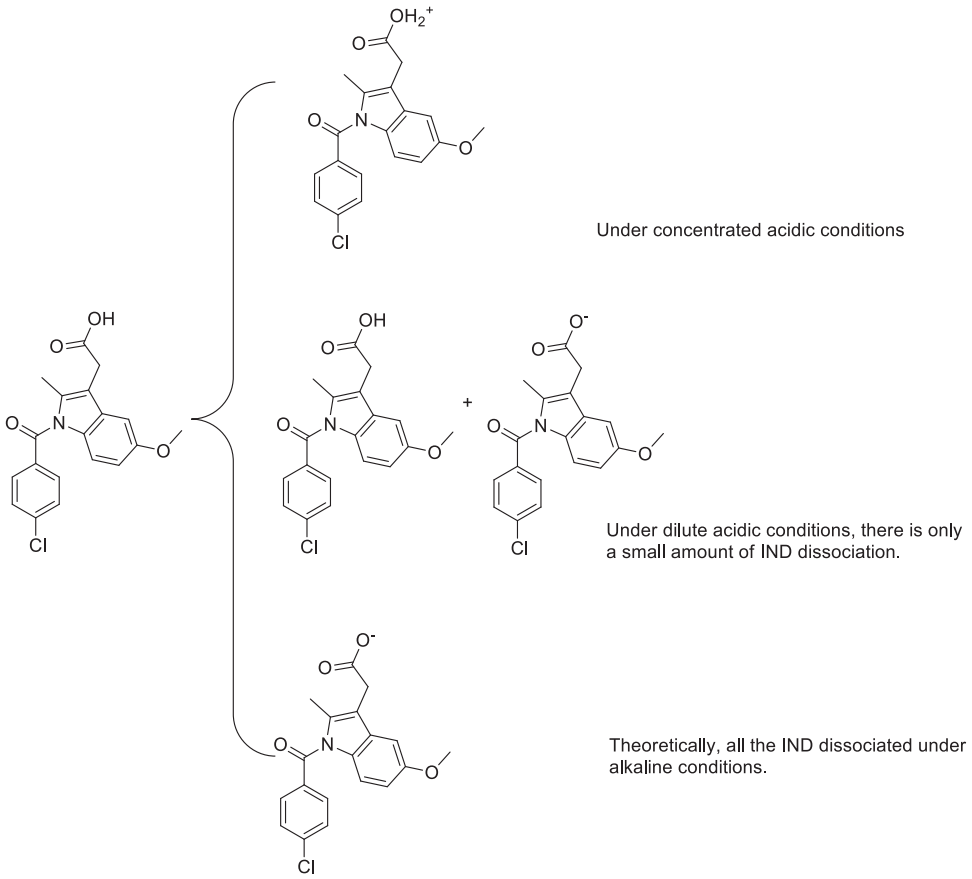

Fig. 8. The dissociation of IND under different pH conditions.

release behavior in the SCF, and the release rate was much faster than that in SGF and SSIF. It was caused by the sensitivity of carboxyl and phenolic hydroxyl groups to alkali, viz., the carboxyl and phenolic hydroxyl groups can be dissociated in the alkaline medium. Moreover, the dissociation of IND under different pH conditions was also an important driving force that influenced the sustained release (Fig. 8). Thus, the obtained DDSs showed significant pH responsiveness. Moreover, the release rate in SGF and SSIF showed a promotion after a period of time (Fig. 7B and C). This phenomenon was generally accompanied by the erosion of OP-DA matrix, resulting in the rupture of emulsion droplets and the acceleration of drug release rate, which was related to the dissociation of carboxyl and phenolic hydroxyl groups under alkali and near-neutral conditions in the present study.

According to SEM (Fig. 6), the emulsion droplet morphology was spherical, and drug release may have various release mechanisms, such as drug diffusion, drug dissolution, and cleavage of chemical bonding for controlled release. Therefore, the drug release behavior was described by commonly used kinetic models such as the First order model, Higuchi model, Ritger-Peppas model, and Bhaskar model. The kinetic fitting curves are shown in Figs. S3–5 (Supporting information), and R^2 and kinetic parameters are recorded in Table S2 (Supporting information). Regression models were commonly used to represent the quality of dynamic models. Under concentrated acid condition (pH=1.2), four models could well describe the release behavior with all R^2 values over 0.95. The fitting results indicated that the drug release mechanism was mainly a diffusion mechanism. The kinetic constant, n, can judge the release mechanism. For spheroidal preparations, n less than 0.45 corresponded to the Fickian diffusion mechanism, n between 0.45 and 0.85 corresponded to the non-Fickian diffusion mechanism, and n greater than 0.85 corresponds to the case II mechanism. The non-Fickian diffusion mechanism was mainly a synergistic effect of diffusion and matrix dissolution, and the case II mechanism was mainly matrix skeleton dissolution. For all the DDSs, the n values were less than 0.43 in the SGF, showing a Fickian diffusion transport. Oppositely, the n values obtained by fitting release data in the SCF and SSIF were all higher than 0.85. Thus, the drug release can be controlled by the skeleton dissolution of OP-DA matrix in diluent acid or alkaline mediums.

3.3. Cytotoxicity assay

The excellent cytocompatibility of materials is the basic condition for biomedical and drug delivery applications. The activity of L929 cells cultured in OP-DAPE was determined by the MTT method, and the cytocompatibility of OP-DAPE was evaluated by observing the fluorescence images. After cultivating L929 cells with the emulsions for 24, 48, and 72 h, the cell viability was assessed. The cell viability of all three samples was higher than 93% after 24 h, as shown in Fig. 9 A-C. According to these results, cell viability was not significantly impacted by the OP-DAPE. The cell viability decreased with the time extension, which may be due to insufficient nutrients inhibiting cell proliferation in the cell culture medium. To better proven the cytotoxicity, the present study collected a much higher concentration (0.0625 mg/mL, 0.125 mg/mL, and 0.25 mg/mL) of OP-DAPE than the published data [52]. Overall, the cell proliferation ratios of the three systems were all above 75% after 72 h of culture, indicating the excellent biocompatibility of the obtained solid particles.

Cell fluorescence staining was employed to observe and analyze the morphology and proliferation of L929 cells exposed to emulsion-based DDS, and the results are shown in Fig. 9 D-F. Most of the L929 cells still showed green fusiform morphology, and the number of cells did not

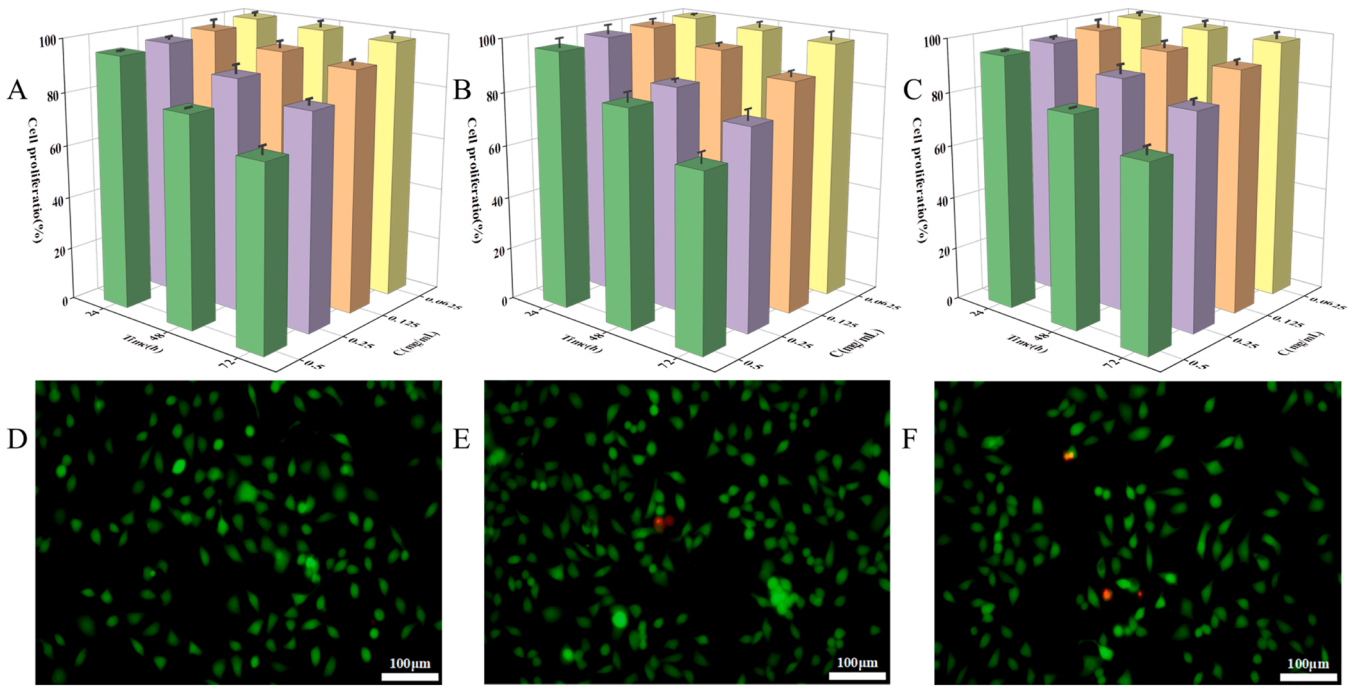

Fig. 9. Cytotoxicity test of OP-DAPE (A-C) and fluorescent images of OP1-DAPE (D-F), where A-C are the L929 cell proliferation under the different initial concentrations of OP1-DAPE, OP2-DAPE, and OP3-DAPE, respectively; D-F are the fluorescent images of cultured L929 cells at the initial concentration of 0.0625 mg/mL of OP1-DAPE sample for 24 h, 48 h, and 72 h.

significantly decrease, indicating great cell proliferation. These results were in accordance with the cell proliferation assay. Thus, the OP-DAPE did not show obvious adverse effects on cell proliferation.

4. Conclusions

In this study, pectin was first oxidized and further functionalized by dopamine to change its hydrophilic properties for forming more stable Pickering emulsions. The obtained OP-DA presented significant differences in wettability, zeta potential, particle size, and PDI values, which contributed to forming stable Pickering emulsions. The particle size of all samples was in the range of 0.358 ± 0.032–0.896 ± 0.144, with a broad particle size diversity. The sample OP1-DA and OP2-DA showed low PDI values of 0.358 ± 0.032 and 0.416 ± 0.031, indicating excellent stabilization capability. SEM observations proved the nano-scale spherical particles of the emulsion droplets. The in vitro drug release showed that the DDS has a low cumulative release ratio of less than 7% in the SGF, and the kinetic studies proved the different release behavior of the emulsion DDS under different pH conditions. The cytocompatibility assay manifested excellent biocompatibility even at a very high concentration of the emulsions. Overall, the present study developed a series of pectin-based Pickering emulsions, which were favorable candidates for delivering water-insoluble drugs.

CRediT authorship contribution statement

Jia-qi Zhang: Conceptualization, Methodology, Resources, Investigation, Formal analysis, Data curation, Writing – original draft. **Haichao Li:** Methodology, Investigation, Data curation, Characterization. **Jie Wang:** Methodology, Resources, Writing – original draft. **Sha-sha Liu:** Methodology, Resources, Investigation, Formal analysis, Data curation. **Jun Li:** Validation, Funding acquisition, Visualization. **Deqiang Li:** Methodology, Validation, Formal analysis, Resources, Writing – original draft, Visualization, Supervision, Funding acquisition.

Declaration of Competing Interest

The authors declare no competing financial interests.

Data availability

Data will be made available on request.

Acknowledgments

The present work was supported by the National Natural Science Foundation of China (No. 32160352), Tianshan Talents Program of Xinjiang, China (2021–2023) (No. 2021267), Postgraduate Innovation Project of Xinjiang Agricultural University (No. XJAUGRI2022048).

Appendix A. Supporting information

Supplementary data associated with this article can be found in the online version at doi:10.1016/j.colsurfa.2023.131807.

References

[1] M. Khotimchenko, Pectin polymers for colon-targeted antitumor drug delivery, Int. J. Biol. Macromol. 158 (2020) 1110–1124.
[2] D. Li, S. Wang, Y. Meng, Z. Guo, M. Cheng, J. Li, Fabrication of self-healing pectin/chitosan hybrid hydrogel via Diels-Alder reactions for drug delivery with high swelling property, pH-responsiveness, and cytocompatibility, Carbohydr. Polym. 268 (2021), 118244.
[3] J.M. Choi, B. Lee, D. Jeong, K.H. Park, E.-J. Choi, Y.-J. Jeon, S.D. Dindulkar, E. Cho, S.H. Do, K. Lee, I.-S. Lee, S. Park, B.-H. Jun, J.-H. Yu, S. Jung, Characterization and regulated naproxen release of hydroxypropyl cyclosophoraose-pullulan microspheres, J. Ind. Eng. Chem. 48 (2017) 108–118.
[4] J. Zhou, Y. Zhai, J. Xu, T. Zhou, L. Cen, Microfluidic preparation of PLGA composite microspheres with mesoporous silica nanoparticles for finely manipulated drug release, Int. J. Pharm. 593 (2021), 120173.
[5] S. Bian, J. Zheng, X. Tang, D. Yi, Y. Wang, W. Yang, One-Pot Synthesis of Redox-Labile Polymer Capsules via Emulsion Droplet-Mediated Precipitation Polymerization, Chem. Mater. 27 (2015) 1262–1268.
[6] S. Zhang, B. Qin, Z. Huang, J.-F. Xu, X. Zhang, Supramolecular emulsion interfacial polymerization, ACS Macro Lett. 8 (2019) 177–182.

[7] E. Villicaña-Molina, E. Pacheco-Contreras, E.A. Aguilar-Reyes, C.A. León-Patiño, Pectin and chitosan microsphere preparation via a water/oil emulsion and solvent evaporation method for drug delivery, Int. J. Polym. Mater. Polym. Biomater. 69 (2019) 467–475.
[8] F. Cui, S. Zhao, X. Guan, D.J. McClements, X. Liu, F. Liu, T. Ngai, Polysaccharide-based Pickering emulsions: Formation, stabilization and applications, Food Hydrocoll. 119 (2021), 106812.
[9] S. Tavasoli, Q. Liu, S.M. Jafari, Development of Pickering emulsions stabilized by hybrid biopolymeric particles/nanoparticles for nutraceutical delivery, Food Hydrocoll. 124 (2022), 107280.
[10] M. López-Pedrouso, J.M. Lorenzo, R. Moreira, D. Franco, Potential applications of Pickering emulsions and high internal-phase emulsions (HIPEs) stabilized by starch particles, Curr. Opin. Food Sci. 46 (2022), 100866.
[11] Y. Shi, F. Ye, Y. Zhu, M. Miao, Development of dendrimer-like glucan-stabilized Pickering emulsions incorporated with beta-carotene, Food Chem. 385 (2022), 132626.
[12] H.M. Ahsan, Y. Pei, X. Luo, Y. Wang, Y. Li, B. Li, S. Liu, Novel stable pickering emulsion based solid foams efficiently stabilized by microcrystalline cellulose/chitosan complex particles, Food Hydrocoll. 108 (2020), 106044.
[13] H. Yan, X. Chen, M. Feng, Z. Shi, W. Zhang, Y. Wang, C. Ke, Q. Lin, Entrapment of bacterial cellulose nanocrystals stabilized Pickering emulsions droplets in alginate beads for hydrophobic drug delivery, Colloids Surf. B Biointerfaces 177 (2019) 112–120.
[14] K. Kamburova, K. Mitarova, T. Radeva, Polysaccharide-based nanocapsules for controlled release of indomethacin, Colloids Surf. A: Physicochem. Eng. Asp. 519 (2017) 199–204.
[15] D. Li, J. Li, H. Dong, X. Li, J. Zhang, S. Ramaswamy, F. Xu, Pectin in biomedical and drug delivery applications: A review, Int. J. Biol. Macromol. 185 (2021) 49–65.
[16] J. Lin, H. Meng, S. Yu, Z. Wang, C. Ai, T. Zhang, X. Guo, Genipin-crosslinked sugar beet pectin-bovine serum albumin nanoparticles as novel pickering stabilizer, Food Hydrocoll. 112 (2021), 106306.
[17] Y. Jiang, Y. Zhu, F. Li, J. Du, Q. Huang, D. Sun-Waterhouse, D. Li, Antioxidative pectin from hawthorn wine pomace stabilizes and protects Pickering emulsions via forming zein-pectin gel-like shell structure, Int. J. Biol. Macromol. 151 (2020) 193–203.
[18] Y. Jiang, Y. Zhu, F. Li, D. Li, Q. Huang, Gliadin/amidated pectin core–shell nanoparticles for stabilisation of Pickering emulsion, Int. J. Food Sci. Technol. 55 (2020) 3278–3288.
[19] J. Yang, L. Liu, Z. Tang, Z. Yang, W. Zhang, Y. Zhu, X. Zeng, L. Zhang, Effect of soybean protein isolate-pectin composite nanoparticles and hydroxypropyl methyl cellulose on the formation, stabilization and lipidolysis of food-grade emulsions, Food Chem. 389 (2022), 133102.
[20] T. Feng, C. Fan, X. Wang, X. Wang, S. Xia, Q. Huang, Food-grade Pickering emulsions and high internal phase Pickering emulsions encapsulating cinnamaldehyde based on pea protein-pectin-EGCG complexes for extrusion 3D printing, Food Hydrocoll. 124 (2022), 107265.
[21] A.-Q. Bi, X.-B. Xu, Y. Guo, M. Du, C.-P. Yu, C. Wu, Fabrication of flavour oil high internal phase emulsions by casein/pectin hybrid particles: 3D printing performance, Food Chem. 371 (2022), 131349.
[22] Z. Li, Y. Xiong, Y. Wang, Y. Zhang, Y. Luo, Low density lipoprotein-pectin complexes stabilized high internal phase pickering emulsions: The effects of pH conditions and mass ratios, Food Hydrocoll. 134 (2023), 108004.
[23] W. Wijaya, S. Turan, A.D. Setiowati, K. Dewettinck, A.R. Patel, P. Van der Meeren, Effect of low-methoxy pectin on interfacial and emulsion stabilizing properties of heated whey protein isolate (WPI) aggregates, Food Structure 26 (2020), 100159.
[24] D. Cheikh, F. Garcia-Villen, H. Majdoub, M.B. Zayani, C. Viseras, Complex of chitosan pectin and clay as diclofenac carrier, Appl. Clay Sci. 172 (2019) 155–164.
[25] S.K. Chinnaiyan, K. Deivasigamani, V.R. Gadela, Combined synergetic potential of metformin loaded pectin-chitosan biohybrids nanoparticle for NIDDM, Int. J. Biol. Macromol. 125 (2019) 278–289.
[26] H. Li, J. Wu, A.S. Doost, J. Su, P. Van der Meeren, Electrostatic interaction between whey proteins and low methoxy pectin studied by quartz crystal microbalance with dissipation monitoring, Food Hydrocoll. 113 (2021), 106489.
[27] K.A. Kristiansen, A. Potthast, B.E. Christensen, Periodate oxidation of polysaccharides for modification of chemical and physical properties, Carbohydr. Res. 345 (2010) 1264–1271.
[28] X. Wei, Z. Zhang, Z. Wang, A simple dopamine detection method based on fluorescence analysis and dopamine polymerization, Microchem. J. 145 (2019) 55–58.
[29] P. Agilan, K. Saranya, N. Rajendran, Bio-inspired polydopamine incorporated titania nanotube arrays for biomedical applications, Colloids Surf. A: Physicochem. Eng. Asp. 629 (2021), 127489.
[30] S.H. Hong, J.H. Ryu, H. Lee, Effect of charge on in vivo adhesion stability of catechol-conjugated polysaccharides, J. Ind. Eng. Chem. 79 (2019) 425–430.
[31] D.-q Li, S.-y Wang, Y.-j Meng, J.-f Li, J. Li, An injectable, self-healing hydrogel system from oxidized pectin/chitosan/gamma-Fe2O3, Int. J. Biol. Macromol. 164 (2020) 4566–4574.
[32] S.A. Ganie, R.A. Naik, A. Ali, T.A. Mir, N. Mazumdar, Preparation, characterization, release and antianemic studies of guar gum functionalized Iron complexes, Int. J. Biol. Macromol. 183 (2021) 1495–1504.
[33] Y. Jiang, Y. Zhu, F. Li, D. Li, Q. Huang, Gliadin/amidated pectin core–shell nanoparticles for stabilisation of Pickering emulsion, Int. J. Food Sci. Technol. 55 (2020) 3278–3288.
[34] Y. Jiang, C. Zhang, J. Yuan, Y. Wu, F. Li, D. Li, Q. Huang, Effects of pectin polydispersity on zein/pectin composite nanoparticles (ZAPs) as high internal-phase Pickering emulsion stabilizers, Carbohydr. Polym. 219 (2019) 77–86.
[35] M.J. Rymaruk, V.J. Cunningham, S.L. Brown, C.N. Williams, S.P. Armes, Oil-in-oil pickering emulsions stabilized by diblock copolymer nanoparticles, J. Colloid Interface Sci. 580 (2020) 354–364.
[36] Y.O. Mezhuev, A.V. Varankin, A.L. Luss, V.A. Dyatlov, A.M. Tsatsakis, M. I. Shtilman, Y.V. Korshak, Immobilization of dopamine on the copolymer of N-vinyl-2-pyrrolidone and allyl glycidyl ether and synthesis of new hydrogels, Polym. Int. 69 (2020) 1275–1282.
[37] C. Rosenbohm, I. Lundt, T.I.E. Christensen, N.G. Young, Chemically methylated and reduced pectins: preparation, characterisation by 1H NMR spectroscopy, enzymatic degradation, and gelling properties, Carbohydr. Res. 338 (2003) 637–649.
[38] P. Perrone, C.M. Hewage, A.R. Thomson, K. Bailey, I.H. Sadler, S.C. Fry, Patterns of methyl and O-acetyl esterification in spinach pectins: new complexity, Phytochemistry 60 (2002) 67–77.
[39] S.-y Wang, Y.-j Meng, J. Li, J.-p Liu, Z.-q Liu, D.-q Li, A novel and simple oral colon-specific drug delivery system based on the pectin/modified nano-carbon sphere nanocomposite gel films, Int. J. Biol. Macromol. 157 (2020) 170–176.
[40] T. Kiss, A. Gergely, Complexes of 3,4-dhydroxyphnyl derivatives, III. Equilibrium study of parent and some mixed ligand complexes of dopamine, alanine and pyrocatechol with nickel(II), copper(II) and zinc(II) ions, Inorg. Chim. Acta 36 (1979) 31–36.
[41] Z. Tai, Y. Huang, Q. Zhu, W. Wu, T. Yi, Z. Chen, Y. Lu, Utility of Pickering emulsions in improved oral drug delivery, Drug Discov. Today (2020).
[42] Q. Guo, J. Su, X. Shu, F. Yuan, L. Mao, J. Liu, Y. Gao, Production and characterization of pea protein isolate-pectin complexes for delivery of curcumin: Effect of esterified degree of pectin, Food Hydrocoll. 105 (2020).
[43] F.-Z. Zhou, X.-N. Huang, Z.-l Wu, S.-W. Yin, J.-h Zhu, C.-H. Tang, X.-Q. Yang, Fabrication of Zein/Pectin Hybrid Particle-Stabilized Pickering High Internal Phase Emulsions with Robust and Ordered Interface Architecture, J. Agric. Food Chem. 66 (2018) 11113–11123.
[44] L. Dai, C. Sun, Y. Wei, L. Mao, Y. Gao, Characterization of Pickering emulsion gels stabilized by zein/gum arabic complex colloidal nanoparticles, Food Hydrocoll. 74 (2018) 239–248.
[45] Y. Jia, J. Li, Molecular assembly of schiff base interactions: construction and application, Chem. Rev. 115 (2015) 1597–1621.
[46] W. Qi, Z. Zhang, T. Wu, Encapsulation of β-carotene in oleogel-in-water Pickering emulsion with improved stability and bioaccessibility, Int. J. Biol. Macromol. 164 (2020) 1432–1442.
[47] Z. Wang, C. Xu, Y. Lu, G. Wei, G. Ye, T. Sun, J. Chen, Microplasma-assisted rapid, chemical oxidant-free and controllable polymerization of dopamine for surface modification, Polym. Chem. 8 (2017) 4388–4392.
[48] S. Arditty, C.P. Whitby, B.P. Binks, V. Schmitt, F. Leal-Calderon, Some general features of limited coalescence in solid-stabilized emulsions, Eur. Phys. J. E Soft Matter 11 (2003) 273–281.
[49] W. Zhang, X. Gu, X. Liu, Z. Wang, Fabrication of Pickering emulsion based on particles combining pectin and zein: Effects of pectin methylation, Carbohydr. Polym. 256 (2021), 117515.
[50] A. Dalmoro, S. Bochicchio, S.F. Nasibullin, P. Bertoncin, G. Lamberti, A.A. Barba, R.I. Moustafine, Polymer-lipid hybrid nanoparticles as enhanced indomethacin delivery systems, Eur. J. Pharm. Sci. 121 (2018) 16–28.
[51] A. Dalmoro, A.Y. Sitenkov, S. Cascone, G. Lamberti, A.A. Barba, R.I. Moustafine, Hydrophilic drug encapsulation in shell-core microcarriers by two stage polyelectrolyte complexation method, Int. J. Pharm. 518 (2017) 50–58.
[52] F. Asabuwa Ngwabebhoh, S. Ilkar Erdagi, U. Yildiz, Pickering emulsions stabilized nanocellulosic-based nanoparticles for coumarin and curcumin nanoencapsulations: In vitro release, anticancer and antimicrobial activities, Carbohydr. Polym. 201 (2018) 317–328.